Excitation of vibrational quanta in water by electron impact

A A A El-Zein, M J Brunger† and W R Newell

Department of Physics and Astronomy, University College London, Gower Street,
London WC1E 6BT, UK

Abstract. A comprehensive study of absolute differential cross sections (DCSs) for electron impact excitation of the bending (010) and unresolved stretching (100 + 001) vibrational quanta of water (H_2O) is reported. Eight incident electron energies (E_0) in the range 6–20 eV were investigated, and the scattered electron angular range was $10°$–$135°$. Integral cross sections (ICSs) were derived from the corresponding vibrational DCSs using a molecular phase shift analysis technique. The self-consistency of these vibrational ICSs was considered by summing them, at each E_0, with available elastic and ionization ICS to provide estimates for the H_2O grand total cross section (GTS), which could then be checked against the independent GTSs of Szmytkowski (1987 *Chem. Phys. Lett.* **136** 363) and Sueoka *et al* (1986 *J. Phys. B: At. Mol. Phys.* **19** L373). Good agreement was typically found.

1. Introduction

At the recent 'electron-driven processes: scientific challenges and technological opportunities' workshop in Hoboken, NJ‡ a group comprised of individuals with expertise in electron-driven processes and individuals with expertise in techniques and methodologies in related fields, met to identify the most promising scientific challenges for the investigation of processes initiated and driven by electron-induced mechanisms. One of the outcomes from this workshop was the identification of water (H_2O) as the prototypical molecule for future, detailed and accurate, theoretical and experimental electron-scattering studies. Consequently, in this paper we report results from one such comprehensive study, specifically an investigation into the excitation of vibrational quanta in H_2O by electron impact.

Previous experimental and theoretical work on electron scattering from H_2O molecules has been well summarized by Johnstone and Newell [1] and Morgan [2], and so we do not repeat those general details again here. However, with respect to the subject matter of this paper, we note the major experimental investigations have been due to Seng and Linder [3, 4], Shyn *et al* [5], Furlan *et al* [6] and a preliminary report of some aspects of the present study [7]. Seng and Linder [4] reported differential cross sections (DCSs), for excitation of both the bending (010) and unresolved stretching (100 + 001) vibrational modes, at nine energies (E_0) in the range 0.35–8 eV. The scattered electron angular range of these measurements was $20°$–$110°$. They also reported excitation functions at the scattered electron angles (θ_e) $20°$ and $90°$ and, in addition, integral cross sections (ICSs) for both the (010) and (100 + 001) modes. Similarly, Shyn *et al* [5] reported DCSs and ICSs for seven energies in the range

---

2.2–20 eV and, again, for both the (010) and (100 + 001) modes. In this case the scattered electron angular range for the DCS measurements was $\theta_e = 30°–150°$. Higher-energy DCS, in this case for $E_0 = 30$ and 50 eV and $\theta_e = 10°–60°$, were measured for (010) and (100 + 001) by Furlan *et al* [6]. As these energies are outside the regime of direct interest for this investigation, we do not discuss their [6] results any further. Finally, we note the work of El-Zein *et al* [7] which concentrated on resonance phenomena in the (010) and (100 + 001) channels in the 6–8 eV impact energy range. DCS and ICS were determined by them at the single-electron energy 7.5 eV, with the angular range of that DCS measurement being $\theta_e = 20°–120°$. The present study significantly extends this earlier work [7] from our group.

From a theoretical perspective the only calculations to go beyond the first Born approximation available in the literature, for vibrational excitation in H_2O, appear to be due to Jain and Thompson [8] and Nishimura and Itikawa [20]. Here DCS and ICS for electron excitation of the symmetric stretch (100), asymmetric stretch (001) and bending modes are detailed.

In this paper, we present absolute DCSs for electron impact excitation of the (010) and (100 + 001) vibrational quanta of H_2O at eight energies in the range 6–20 eV. The scattered electron angular range is $10°–135°$. A molecular phase shift analysis procedure [7, 9] is then applied to these DCSs to enable us to derive the corresponding ICSs. In the next section of this paper a brief precis of the apparatus and experimental techniques is given. In section 3 our results are presented and discussed, while in section 4 some conclusions from the current investigation are drawn.

2. Experimental details

The electron spectrometer and measurement procedures used in the current crossed-beam work are essentially those used in Johnstone *et al* [10], and so only a cursory description of the relevant details is given here. A beam of H_2O, effusing from a titanium tube of internal diameter 0.5 mm and length 10 mm, is crossed with a beam of mono-energetic electrons of desired energy E_0. In the present application $E_0 = 6, 7.5, 8.75, 10, 12.5, 15, 17.5$ and 20 eV. Elastically and inelastically scattered electrons at a particular scattering angle are energy analysed and detected by a channel electron multiplier. The overall energy resolution for these experiments is typically 50 meV (FWHM) and, under normal operating conditions, incident electron beam currents ~ 2 nA were obtained in the interaction region.

At each scattering angle and energy, energy-loss spectra were recorded over the range $-0.3–0.6$ eV. A typical spectrum at $E_0 = 7.5$ eV and $\theta_e = 30°$ is shown in figure 1 (see also [7]). Three peaks can be identified in this spectrum. They are due to elastic scattering (000) and electron impact excitation of the (010) and (100 + 001) fundamental vibrational quanta of H_2O. The spectra were obtained by applying a linear voltage ramp to the reference rail (energy loss) of the electron optic and hemispherical energy analysis elements, that constitute the analyser, in an energy-loss mode in conjunction with a computer-based multichannel scaler which stored the scattered signal as a function of energy loss. Each spectrum was then analysed to determine the ratio R (from the areas A under the respective peaks) of the inelastic to elastic intensities,

$$R_k(\theta_e) = \frac{A_k(\theta_e)}{A_{\text{elastic}}(\theta_e)} \qquad \text{for all } k = (010) \text{ or } (100 + 001). \tag{1}$$

Provided the transmission of the scattered electron analyser is well characterized [11] this ratio is equivalent to the ratio of the DCS for the vibrational excitation process of interest
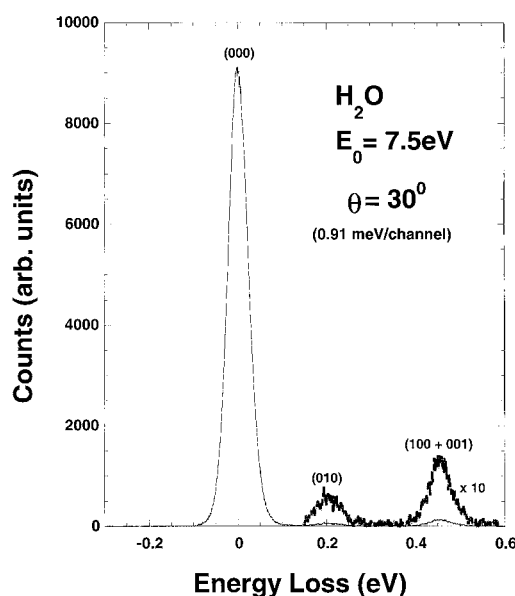
Figure 1. Typical energy-loss spectrum for $e^- + H_2O$ scattering. The present data (●) and an interpolation through those data (—) are shown. The incident electron energy is 7.5 eV and the electron scattering angle is 30°. The positions of the excited vibrational quanta are indicated in the figure.

$(\sigma_k(\theta_e))$ to that for elastic scattering $(\sigma_0(\theta_e))$,

$$R_k(\theta_e) = \frac{\sigma_k(\theta_e)}{\sigma_0(\theta_e)} \qquad \text{for all } k = (010) \text{ or } (100 + 001). \qquad (2)$$

It follows from equation (2) that, provided $\sigma_0(\theta_e)$ is known, the relevant inelastic DCS can be derived. In the current study we have employed the absolute elastic DCSs of Johnstone and Newell [1], or an interpolation from those data, to determine the required values for $\sigma_{(010)}(\theta_e)$ and $\sigma_{(100+001)}(\theta_e)$, respectively. Note that our interpolation of the data of Johnstone and Newell [1], to obtain values for the DCS at energies they did not specifically measure, is valid in this case because of the absence of resonance behaviour in the elastic channel [1, 12] in the energy regime we consider.

Careful consideration has been given to the optimization of the transmission of the post-collision electron optics [10] in these measurements. This is crucial to enable accurate determinations for $R_k(\theta_e)$. The maximum energy difference for the electrons is around 0.46 eV (the energy difference between elastic scattering and the (100 + 001) vibrational excitation), which at an incident energy of 6 eV represents a change of only 7.5% in the scattered electron energy.

A general discussion of the errors associated with the present type of measurements can be found in Nickel *et al* [13]. In the current work the statistical errors associated with the scattering intensity measurements are small (< 5%). Additional errors due to the uncertainty in the elastic differential cross sections [1] (~ 13–17%) and an uncertainty in the uniformity of our analyser transmission (conservatively estimated to be ~ 10%) must also be considered. When these sources of error are added together in quadrature we find an overall error on our (010) DCSs to be typically ~ 19.5%, and an overall error on our (100 + 001) DCSs to be typically ~ 18.8%.
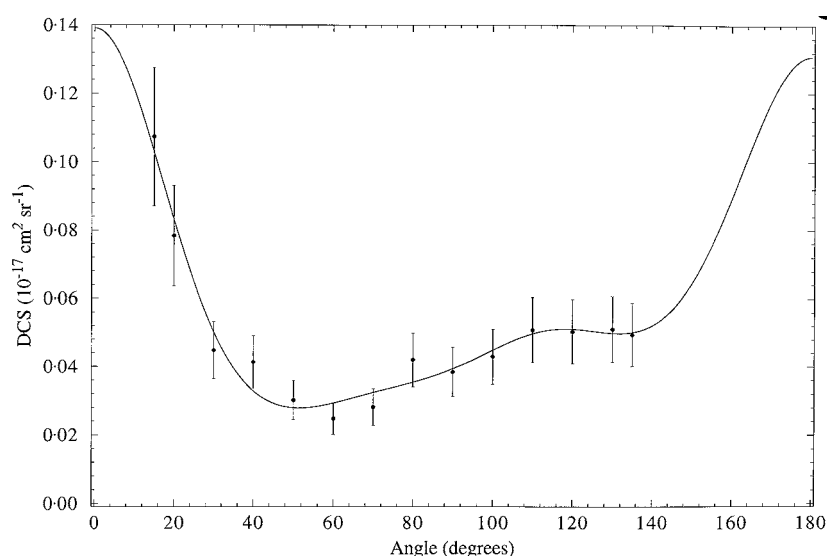
Figure 2. Result of the MPSA procedure fit (——) to the present 20 eV (100 + 001) differential cross section (●) data. Seven partial waves were allowed to vary in this fit, with higher-order terms obtained from the Born series result.

To derive ICSs from our DCS measurements we have applied the molecular phase shift analysis (MPSA) procedure of Boesten and Tanaka [9] (and references therein), to the respective (010) and (100 + 001) DCSs. A typical result of this process for the (100 + 001) modes at $E_0 = 20$ eV is given in figure 2. It is clear from figure 2 that the MPSA gives an excellent fit to the measured differential cross section and provides a plausible extrapolation to 0° and 180°. This extrapolation is then used in conjunction with the measured DCS to calculate the integral,

$$I_k(E_0) = \int_0^\pi \sigma_k(E_0, \theta) \sin \theta \, d\theta. \tag{3}$$

The relevant integral cross section is then found in the standard manner from

$$Q_k(E_0) = 2\pi I_k(E_0). \tag{4}$$

In the present application of the MPSA usually around seven partial waves are allowed to vary in the fit to our measured DCS. Higher-order partial waves were accounted for using the Born series result [9, 14].

## 3. Results and discussion

3.1. Differential cross sections

In tables 1 and 2 we present our differential cross sections for electron impact excitation of the (010) and (100 + 001) vibrational quanta of H_2O, respectively. A representative selection of these DCSs is also plotted in figures 3(*a*)–(*c*) and figures 4(*a*)–(*c*). Note that in both these series of plots (*a*) corresponds to a 6 eV incident electron energy, (*b*) corresponds to a 10 eV incident electron energy and (*c*) corresponds to a 15 eV incident electron energy.

Considering figure 3 in more detail we see that the shape of the (010) differential cross section changes significantly as the energy of the incident electron beam is increased. It is
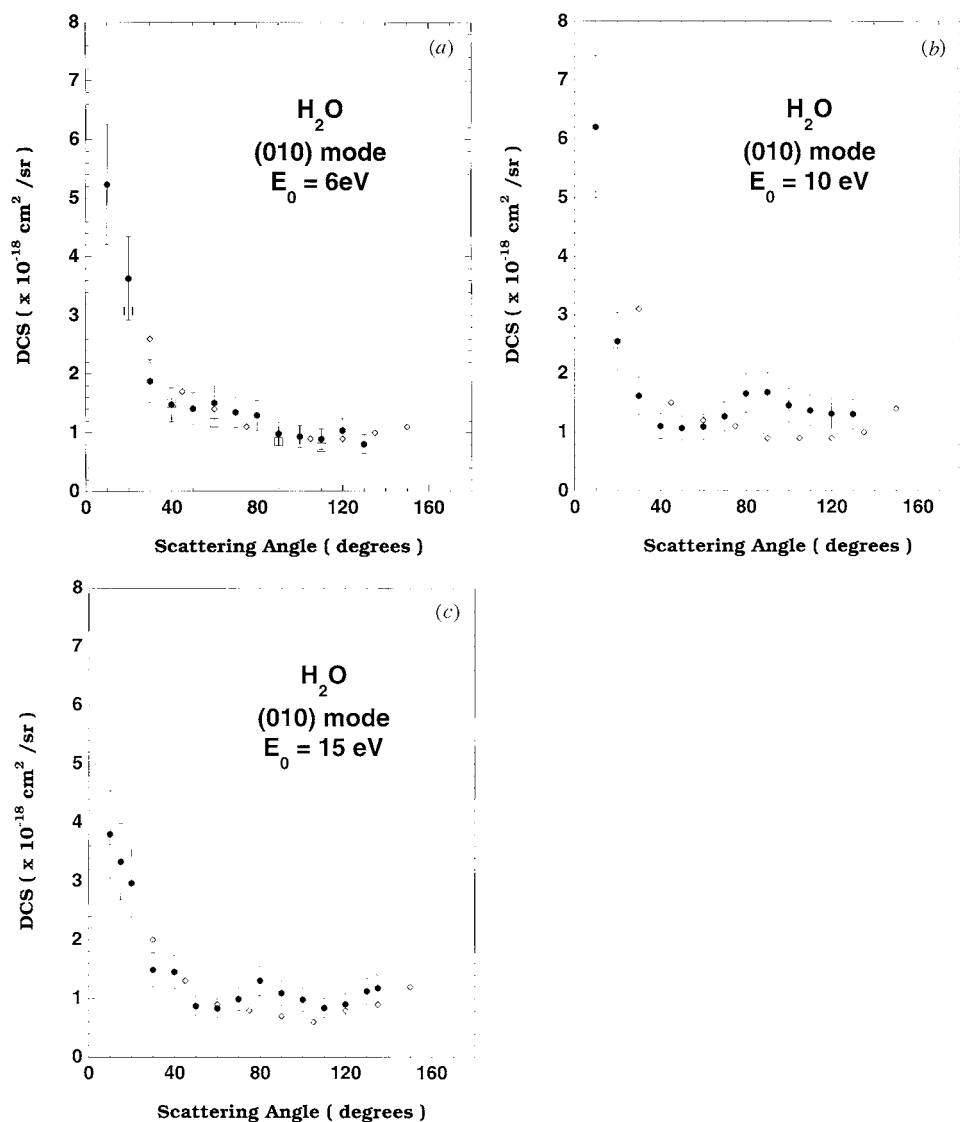
Figure 3. Differential cross sections ($\times 10^{-18}$ cm^2 sr^{-1}) for electron impact excitation of the (010) vibrational mode of water at (*a*) 6 eV, (*b*) 10 eV and (*c*) 15 eV. The present data (●) are compared with the previous results of: □, Seng and Linder [4] and ◇, Shyn *et al* [5].

clear from figures 3(*a*)–(*c*) that while all the differential cross sections are strongly peaked in the forward scattered electron angle direction, indicating the importance of the electron–dipole-moment interaction for excitation of this mode, it is also apparent that although at 6 eV there is essentially no angular structure in the DCS, at 10 and 15 eV there is important angular structure at middle angles. This angular structure, or enhancement of the DCS, at 10 and 15 eV and middle angles is due to resonant decay of a B-symmetry state of H$_2$O$^-$ into the (010) channel. This point was examined in detail earlier by El-Zein *et al* [7] and so we do not repeat those arguments again here. Note, however, the conclusions drawn by El-Zein *et al* are entirely consistent with the results of the calculation of Jain and Thompson [8] as to the
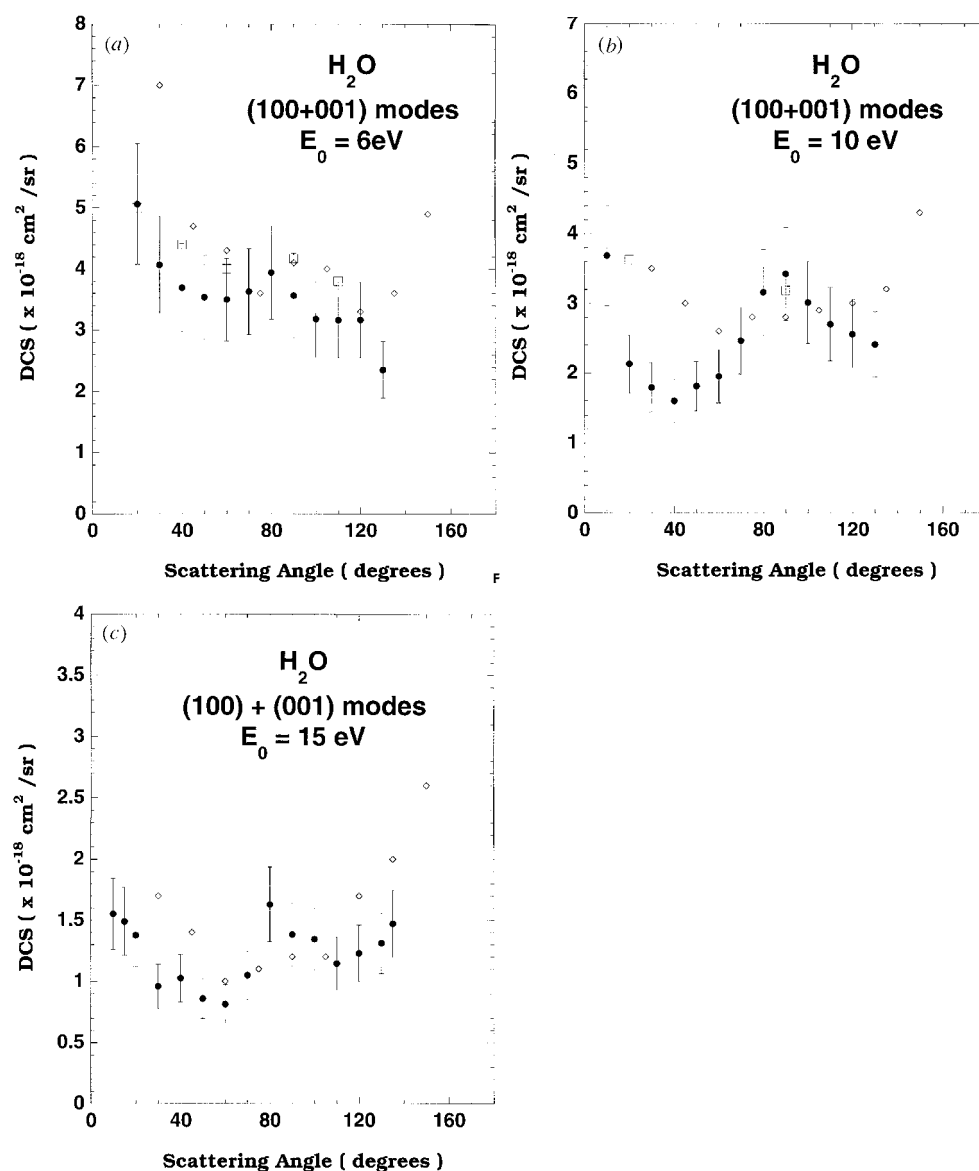
Figure 4. Differential cross sections ($\times 10^{-18}$ cm^2 sr^{-1}) for electron impact excitation of the (100 + 001) vibrational modes of water at (*a*) 6 eV, (*b*) 10 eV and (*c*) 15 eV. The present data (●) are compared with the previous results of: □, Seng and Linder [4] and ◇, Shyn *et al* [5].

symmetry of the resonant state and that it decays into both the bending and stretching modes of water. When we compare the present (010) DCS with those of other workers, then at 6 eV (figure 3(*a*)) the level of agreement between our work and that of both Seng and Linder [4] and Shyn *et al* [5] is generally very good across the entire common angular range of measurement. At 10 eV, however, this is not the case (figure 3(*b*)). The angular distribution of Shyn *et al* [5] is more strongly peaked at forward scattering angles than the present result, and it also has none of the angular structure of the current measurement. For 10 eV incident electrons

Table 1. Differential cross sections ($\times 10^{-18}$ cm^2 sr^{-1}) for electron impact excitation of the (010) vibrational quantum in H$_2$O. The error on the present data is typically $\sim \pm 19.5\%$ at each energy.

θ (deg)	E_0 (eV)							
	6.0	7.5	8.75	10.0	12.5	15.0	17.5	20.0
10	5.231	4.610	5.923	6.204	—	3.801	6.703	—
15	—	—	—	—	3.637	3.336	3.452	2.949
20	3.631	2.600	3.053	2.543	1.972	2.966	2.448	2.151
30	1.876	1.970	2.030	1.619	1.618	1.487	1.439	1.281
40	1.476	1.870	1.532	1.102	1.634	1.449	1.106	1.067
50	1.407	2.330	1.250	1.069	1.078	0.871	0.867	0.657
60	1.504	2.390	1.444	1.091	1.240	0.830	0.862	0.559
70	1.344	2.320	1.330	1.265	1.139	0.988	0.746	0.560
80	1.295	2.100	1.143	1.661	1.319	1.302	0.909	0.641
90	0.982	2.110	0.964	1.680	1.103	1.080	0.753	0.545
100	0.936	1.600	0.869	1.457	0.850	0.980	0.931	0.611
110	0.894	1.450	1.046	1.369	0.864	0.842	0.899	0.762
120	1.036	1.510	0.922	1.314	0.982	0.905	1.013	0.847
130	0.807	—	0.933	1.305	1.010	1.124	0.846	0.874
135	—	—	—	—	0.867	1.178	0.924	0.919

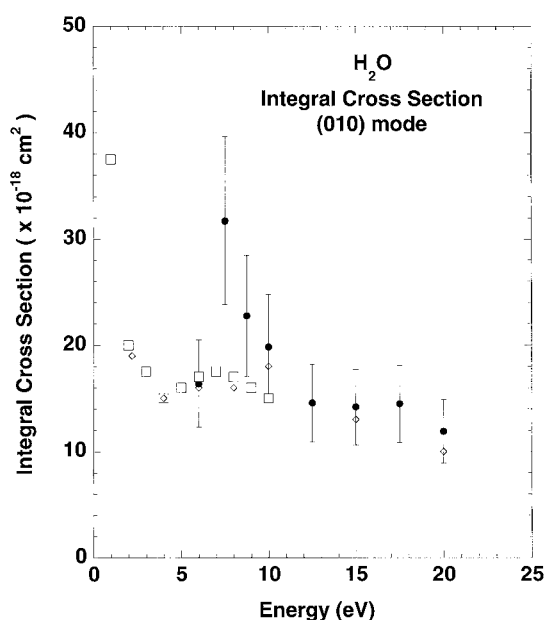**Table 2.** Differential cross sections ($\times 10^{-18}$ cm^2 sr^{-1}) for electron impact excitation of the (100 + 001) vibrational quanta in H$_2$O. The error on the present data is typically $\sim \pm 18.8\%$ at each energy.

θ (deg)	E_0 (eV)							
	6.0	7.5	8.75	10.0	12.5	15.0	17.5	20.0
10	—	5.630	3.263	3.685	—	1.553	2.624	—
15	—	—	—	—	1.808	1.491	1.393	1.073
20	5.062	5.230	2.876	2.127	1.345	1.376	0.994	0.783
30	4.068	4.230	2.603	1.793	1.561	0.960	0.690	0.447
40	3.695	4.230	2.317	1.597	1.608	1.025	0.659	0.412
50	3.534	4.940	2.270	1.809	1.414	0.860	0.599	0.301
60	3.497	5.280	2.646	1.949	1.615	0.817	0.581	0.247
70	3.628	5.360	2.706	2.461	1.651	1.050	0.597	0.281
80	3.941	5.570	2.708	3.156	2.195	1.630	0.794	0.419
90	3.562	5.250	2.765	3.420	2.053	1.383	0.819	0.384
100	3.178	4.340	2.587	3.008	1.886	1.344	0.757	0.429
110	3.162	3.340	2.370	2.699	1.802	1.145	0.695	0.507
120	3.164	3.640	2.354	2.556	1.650	1.228	0.717	0.502
130	2.354	—	2.084	2.407	1.619	1.312	0.571	0.509
135	—	—	—	—	1.307	1.471	0.820	0.493

we only have the $\theta_e = 20°$ and $90°$ DCS of Seng and Linder [4] (from their (010) excitation function measurement) to compare with our results. In this case the $\theta_e = 20°$ datum point of Seng and Linder is in excellent agreement with the current DCS, although at $90°$ the agreement between us is quite poor. This discrepancy at $90°$ simply reflects the following point. Namely, that Seng and Linder found the dominant population mechanism for the (010) mode was due to direct scattering, while we additionally observe an important resonant enhancement effect. The present 15 eV DCS is plotted in figure 3(*c*), where we can only compare with the result of Shyn *et al* [5]. It is apparent from figure 3(*c*) that for $\theta_e \leqslant 60°$ and $\theta_e \geqslant 110°$ the present

DCSs and those of Shyn *et al* are in quite good accord. At middle angles, however, the level of agreement is only marginal, although it is true that to within the combined uncertainties on the two respective data sets there should be overlap between them. While we do not specifically plot the 20 eV DCS for excitation of the (010) quantum, we note that at this energy the shape of the present angular distribution is essentially structureless, as is expected away from the influence of the decay of the H_2O^- state.

Electron impact excitation of the (100 + 001) stretching modes of water are considered in figures 4(*a*)–(*c*). At each of these respective energies the cross sections are forward peaked, although the degree of forward peaking in the angular distributions is significantly less than that found previously at the corresponding energy for the (010) mode (see figures 3(*a*)–(*c*)). On the other hand, the amount of angular structure in each of the illustrated (100 + 001) DCS is significantly stronger than that seen *vis-à-vis* for the (010) mode. These observations are consistent with the resonant decay process, from the B-symmetry state of H_2O^-, playing a more significant role in the excitation of the stretching modes than was found for the bending mode. They also indicate (see figures 4(*a*)–(*c*)) the comparatively smaller effect that direct scattering has for excitation of the stretching modes than for excitation of the bending mode. The agreement between the present data and those of Seng and Linder [4] for excitation of the (100 + 001) modes is, at the common energies of measurement, very good. This is specifically illustrated in figure 4(*a*). Indeed, both the current DCSs and those of Seng and Linder show significant angular structure at middle electron scattering angles (see also [7]), consistent with resonance enhancement of the cross sections. On the other hand, the DCSs of Shyn *et al* [5] exhibit no angular structure in any of their (100 + 001) angular distributions (see figures 4(*a*)–(*c*)). Consequently, the agreement between the present data and those of Shyn *et al* is generally quite marginal, the earlier DCS work [5] having a different shape and often tending to be stronger in magnitude at both the more forward and backward scattering angles.

Figure 5. Integral cross sections ($\times 10^{-18}$ cm^2) for electron impact excitation of the (010) vibrational mode of water. The present data (●) are compared with the previous results of: □, Seng and Linder [4] and ◇, Shyn *et al* [5].
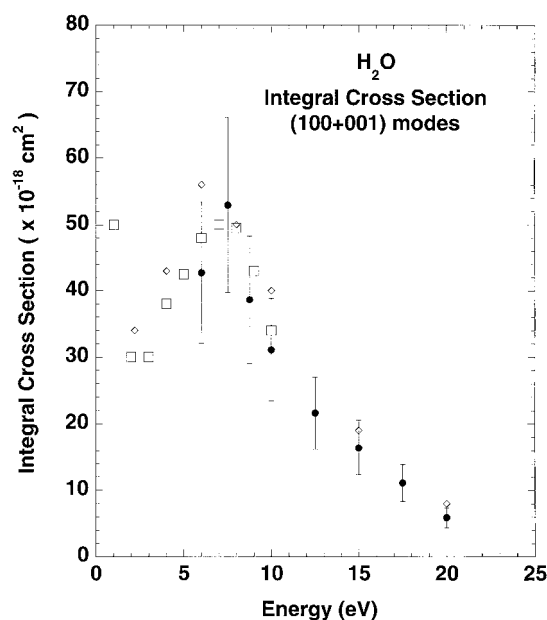
Figure 6. Integral cross sections ($\times 10^{-18}$ cm^2) for electron impact excitation of the $(100 + 001)$ vibrational modes of water. The present data ($\bullet$) are compared with the previous results of: $\square$, Seng and Linder [4] and $\diamond$, Shyn *et al* [5].

3.2. Integral cross sections

In tables 3 and 4 we present our integral cross sections for electron impact excitation of the (010) and $(100+001)$ vibrational quanta of H_2O, respectively. These ICS are also plotted in figure 5, for the (010) mode, and figure 6, for the $(100 + 001)$ modes. Recall that the present ICS were determined from our DCS measurements using the MPSA procedure discussed in section 2. It is obvious from figures 5 and 6 that the current measurements confirm the preliminary conclusion of El-Zein *et al* [7], namely that the broad B-symmetry shape resonance of H_2O^- enhances both the (010) and $(100 + 001)$ cross sections in the ≈ 6–10 eV energy range. We again highlight the consistency of this result with that obtained from their calculations by Jain and Thompson [8] and Nishimura and Itikawa [20].

Table 3. Integral cross sections ($\times 10^{-18}$ cm^2) for electron impact excitation of the (010) vibrational quantum in H_2O. The error on the present data is $\sim \pm 25\%$.

E_0 (eV)	ICS ($\times 10^{-18}$ cm^2)
6.0	16.37
7.5	31.70
8.75	22.73
10.0	19.82
12.5	14.55
15.0	14.17
17.5	14.47
20.0	11.88

Table 4. Integral cross sections ($\times 10^{-18}$ cm^2) for electron impact excitation of the (100 + 001) vibrational quanta in H$_2$O. The error on the present data is $\sim \pm 25\%$.

E_0 (eV)	ICS ($\times 10^{-18}$ cm^2)
6.0	42.72
7.5	52.90
8.75	38.62
10.0	31.06
12.5	21.61
15.0	16.41
17.5	11.11
20.0	5.913
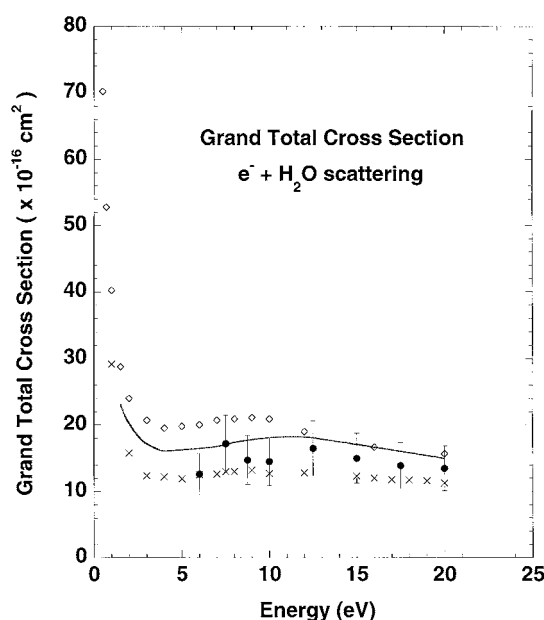
Figure 7. Grand total cross sections ($\times 10^{-16}$ cm^2) for electron scattering from water. The present data ($\bullet$) are compared with the previous results of: ——, Brüche [16]; $\diamond$, Szymtkowski [17]; and $\times$, Sueoka *et al* [18].

Considering figure 5 in more detail we note that at $E_0 = 6$ eV and for $E_0 \geqslant 10$ eV all the available (010) ICS measurements are, to within their respective experimental uncertainties, in good agreement with one another. In the region of the resonance, however, the present (010) ICSs are significantly larger in magnitude than those of either Seng and Linder [4] or Shyn *et al* [5], which are themselves in quite good accord. Indeed, at the peak ($E_0 \sim 7.5$ eV) of the resonance the present (010) ICS is almost a factor of two greater in magnitude than that of Seng and Linder and Shyn *et al*. The possible origin for this discrepancy was examined by El-Zein *et al* [7], although no definitive conclusions were drawn by them. Given, as we shall see shortly, the very good agreement between all three data sets, to within their errors, for the (100 + 001) ICSs the origin of this discrepancy, at and near resonance, in the (010) mode ICS remains something of a mystery.

Table 5. Integral elastic cross sections ($\times 10^{-16}$ cm^2) for e$^-$ + H_2O scattering. The 'present' elastic ICS were derived by applying a MPSA to the earlier work of Johnstone and Newell [1]. The error on the 'present' elastic ICS is ±20%.

E_0 (eV)	ICS ($\times 10^{-16}$ cm^2)
6.0	11.98
7.5	16.34
8.75	14.07
10.0	13.96
12.5	16.16
15.0	14.57
17.5	13.36
20.0	12.83

Table 6. Grand total cross sections ($\times 10^{-16}$ cm^2) for e$^-$ + H_2O scattering. The error on the present GTS is ±25%. Note that the ionization cross section for H_2O was taken from Kim and Rudd [15], (see text).

E_0 (eV)	ICS ($\times 10^{-16}$ cm^2)
6.0	12.6
7.5	17.2
8.75	14.7
10.0	14.5
12.5	16.5
15.0	15.0
17.5	13.9
20.0	13.5

The present (100 + 001) integral cross sections are plotted in figure 6, along with the earlier results of Seng and Linder [4] and Shyn *et al* [5]. The agreement, as alluded to above, between all three data sets is very good across the entire common energy regimes. Thus an 'optimum' experimental cross section set for excitation of the (100 + 001) modes could easily be derived from the three existing ICS measurements. This 'optimum' set would then provide theorists with a benchmark ICS for this process, against which they could test the validity of their calculations.

In table 5 we provide the integral elastic cross sections that we have derived, using the MPSA, from the elastic DCS measurements of Johnstone and Newell [1]. Note that in all cases the present estimates for the elastic ICS are consistent with those provided earlier by Johnstone and Newell, thereby demonstrating the utility of the MPSA procedure. When the elastic ICSs of table 5 are combined with the vibrational ICSs from tables 3 and 4, at each E_0, and the corresponding ionization cross sections for water from Kim and Rudd [15] we are able to obtain a lower bound estimate of the grand total cross section (GTS) for e$^-$ + H_2O scattering. The results of this process are tabulated in table 6 and plotted in figure 7. Also shown in figure 7 are the previous GTS determinations from Brüche [16], Szmytkowski [17] and Sueoka *et al* [18]. Note that the present GTS estimates are a lower bound on the true values because they do not include ICSs for excitation of any of the electronic states of H_2O [19], for which absolute values are unavailable in the literature. Nonetheless it is clear from figure 7 that the current GTS values are in reasonable accord with the other available independent experimental data [16–18]. Consequently, we can surmise that the present elastic and vibrational ICS, when summed with reliable ionization

ICS from Kim and Rudd [15], provide a self-consistent set for electron scattering from H_2O.

4. Conclusions

We have reported on a comprehensive investigation into electron impact excitation of the (010) and (100 + 001) vibrational quanta in water. Important resonant enhancement effects in both these modes were observed in the ~ 6–10 eV impact energy range. The present DCS and ICS data, when combined with the lower-energy results of Seng and Linder [4], provide an extensive and accurate body of data, from near threshold to 20 eV, against which state-of-the-art electron–polyatomic molecule scattering theories can benchmark their calculations.

This paper therefore satisfies one of the outcomes of the recent Hoboken meeting which established H_2O as the prototypical molecule to be jointly studied in depth by theoreticians and experimentalists.

Acknowledgments

References

[1] Johnstone W M and Newell W R 1991 *J. Phys. B: At. Mol. Opt. Phys.* **24** 3633
[2] Morgan L 1998 *J. Phys. B: At. Mol. Opt. Phys.* **31** 5003
[3] Seng G and Linder F 1974 *J. Phys. B: At. Mol. Phys.* **7** L509
[4] Seng G and Linder F 1976 *J. Phys. B: At. Mol. Phys.* **9** 2539
[5] Shyn T, Cho S Y and Cravens T E 1988 *Phys. Rev.* A **38** 678
[6] Furlan M, Hubin-Franskin M-J, Delwiche J and Collin J E 1991 *J. Chem. Phys.* **95** 1671
[7] El-Zein A, Brunger M J and Newell W R 2000 *Chem. Phys. Lett.* **319** 701
[8] Jain A and Thompson D G 1983 *J. Phys. B: At. Mol. Phys.* **16** L347
[9] Boesten L and Tanaka H 1991 *J. Phys. B: At. Mol. Opt. Phys.* **24** 821
[10] Johnstone W M, Akther P and Newell W R 1995 *J. Phys. B: At. Mol. Opt. Phys.* **28** 743
[11] Brunger M J and Buckman S J 1997 *Nucleaus* **34** 201
[12] Shyn T W and Cho S Y 1987 *Phys. Rev.* A **36** 5138
[13] Nickel J C, Zetner P W, Shen G and Trajmar S 1989 *J. Phys. E: Sci. Instrum.* **22** 730
[14] Merz R and Linder F 1998 *J. Phys. B: At. Mol. Opt. Phys.* **31** 4663
[15] Kim Y-K and Rudd M E 1994 *Phys. Rev.* A **50** 3954
[16] Brüche E 1927 *Ann. Phys., Lpz.* **82** 25
[17] Szmytkowski C 1987 *Chem. Phys. Lett.* **136** 363
[18] Sueoka O, Mori S and Katayama Y 1986 *J. Phys. B: At. Mol. Phys.* **19** L373
[19] Trajmar S, Williams W and Kupperman A 1973 *J. Chem. Phys.* **58** 2521
[20] Nishimura T and Itikawa Y 1995 *J. Phys. B: At. Mol. Opt. Phys.* **28** 1995